Winter 1-15-2019

Combination of gold nanoparticles with low-LET irradiation: an approach to enhance DNA DSB induction in HT29 colorectal cancer stem-like cells

Mahdi Abbasian
Stem Cell Research CenterGolestan University of Medical ScienceGorgānIran

Zahra Arab-Bafrani
Stem Cell Research CenterGolestan University of Medical ScienceGorgānIran, arabbafrani@goums.ac.ir

Azam Baharlouei
Southern Illinois University Carbondale

David Lightfoot
Southern Illinois University Carbondale

Recommended Citation

Abbasian, Mahdi, Arab-Bafrani, Zahra, Baharlouei, Azam and Lightfoot, David. "Combination of gold nanoparticles with low-LET irradiation: an approach to enhance DNA DSB induction in HT29 colorectal cancer stem-like cells." *Journal of Cancer Research and Clinical Oncology* 145, No. 1 (Winter 2019): 97–107. doi:10.1007/s00432-018-2769-3.

Gold nanoparticles enhance the radiobiological effects of low LET irradiation on HT29 colon cancer stem like cells

Mahdi Abbasian[1, 2] Azam Baharlouei[2, 3], Zahra Arab-Bafrani[1, 4*], Elham Mosavi[5], David A. Lightfoot[6]

[1] Stem Cell Research Center, Golestan University of Medical Science, Gorgan, Iran.

[2] Department of Biotechnology, College of Agriculture, Isfahan University of Technology, Isfahan, Iran.

[3] Department of Microbiology, Southern Illinois University at Carbondale, Carbondale, IL 62901, USA

[4] Department of Medical Physics, School of Medicine, Golestan University of Medical Sciences, Gorgan, Iran.

[5] Health Research Institute, Infectious and Tropical Diseases Research Center, Ahvaz Jundishapur University of Medical Sciences, Ahvaz, Iran

[6] Department of Plant, Soil and Agricultural Systems, Plant Biotechnology and Genome Core-Facility, Southern Illinois University at Carbondale, Carbondale, IL 62901, USA

*__Corresponding author__: Zahra Arab-Bafrani, Department of Medical Physics, School of Medicine, Golestan University of Medical Sciences, Gorgan, Iran, arabbafrani@goums.ac.ir

Abstract

High-linear energy transfer (High LET) irradiation has significant cytotoxic effects on different cancerous, stem-like, cells (CSLCs) such as colon CSLCs. A review of the literature has indicated that the presence of gold nanoparticles (GNPs) enables low LET irradiation to produce a highly non-homogeneous dose distributions like high LET irradiation.The purpose of this study was to evaluate the radio-responsiveness of HT29 colon CSLCs under low LET irradiation (X-ray) and in the presence of GNPs.Radio-responsiveness was evaluated using the ϒ-H2AX foci formation assay, the clonogenic assay, the cell cycle progression assay and analyses of radiobiological parameters.In the presence of GNPs, the survival fraction of HT29 CSCLs was significantly reduced, and caused significant changes in the radiobiological parameters after irradiation. In addition, ϒ-H2AX assay showed that in the presence of GNPs, the persistent DNA double strand breaks (DSBs) were significantly increased in irradiated HT29 CSLCs. The relative biological effectiveness (RBE) value of GNPs with X-rays was about 1.6 for HT-29 CSLCs at the D10 stage when compared to X-rays alone. Therefore, the combination of GNPs with X-ray irradiation has potential to kill HT29 CSLCs greater than the X-rays alone, and may be considered as an alternative for high LET irradiation.

Keyword: High LET, gold nanoparticle, cancer stem-like cell, DNA double-strand breaks

Introduction

Despite all the recent developments in cancer therapy, colorectal cancer recurrence is still a crucial problem, and the reason for this phenomenon is not fully understood (1,2). Many studies support the hypothesis implies that cancer stem-like cells (CSLCs) contribute to the recurrence of the tumor (3,4). Given the important role of colorectal CSLCs in the failure of conventional radiotherapy, designing a new radiotherapeutic strategy is imperative to aid colorectal CSLCs elimination.

Based on recent studies, high-linear energy transfer (High LET) irradiation has various advantages (1-4). These include increased relative biological effectiveness (RBE), less cell cycle dependency and inducing unrepairable double strand breaks (DSB) comparing to low LET irradiation, X-ray energy (5,6). In the recent reports, it has been demonstrated that High LET irradiation increases killing effects on the CSLCs of colorectal (2), pancreatic (7), glioblastoma (6,8), human tongue (9) and breast (10) cells. However, expensive establishment of high LET caused some limitations to access this modality (2,11). Therefore, the improvement of conventional radiotherapy effects by using some strategies such as application of a radiosensitizer can be considered as an effective and affordable method.

In the last decade, gold nanoparticles (GNPs) were presented as good radiosensitizers owing to an increased absorption dose of radiation. Based on the recent nano-dosimetry model, in addition to the production of relatively high energy Photo and Compton electrons, interaction between radiation and GNPs produce a number of secondary electrons (12). These electrons include a shower of low energy and small range Auger electrons that deposit their energy in the vicinity of the GNPs and cause highly inhomogeneous dose distributions on the nanoscale. A combination of extremely high absorbed doses and exceedingly small volumes is the common characteristic that can be frequently seen around particle tracks in high LET irradiation (13). Consistently, our previous study showed that the enhancement of absorbed dose in HT29 cancer cells under low LET (9MV X-ray) irradiation in the presence of GNPs

(14). Moreover, several studies showed that in the presence of GNPs, the number of ϒ-H2AX foci was increased in irradiated cancer cells which was due to an increased DNA DSBs (15–17).

Based on these evidences, we hypothesized that the combination of GNPs and low LET irradiation may efficaciously target CSLCs. To this end, we first evaluated the resistance mechanism of HT29 CSLCs to the low LET irradiation through radiobiological parameters, cell cycle progression, cell cycle redistribution and the number of induced DNA DSBs. In this study, the changes in above mentioned parameters were assessed in the presence of GNPs. To the best of our knowledge, this study is the first to explore whether the combination of GNPs and X-ray irradiation can enhance radiosensitization of HT29 CSLCs and may be considered as an alternative to high LET irradiation.

Methods

Cell culture

Colorectal (HT29) cell line was purchased from Pasteur Institute (Tehran, Iran). Cells were cultured in RPMI1640 (Gibco-Invitrogen) supplement by 10% fetal bovine serum, (Gibco-Invitrogen) and 1% penicillin/streptomycin (Sigma- Aldrich). The cells were incubated at humidified atmosphere in 37 °C with 5% CO2. The cells' medium was changed every two days. In order to isolate CSLCs with ability to form spheroid like structure, parental cells subcultured in serum free DMEM/F12 medium (SFM) on collagen type I coated plates (Col/SFM) as reported previously (18–20). The morphological changes of HT29 cells and formation of spheroid in Col/SFM at various time points investigated with an inverted microscopy (Nikon TS100). Also, for viewing the three dimensional conformation of HT29 spheroid on collagen coated plate using a scanning electron microscopy (SEM), samples were prepared as previously reported (21). HT29 CSLCs and parental cells were incubated with

final concentration of 80 µM GNPs, 24 h before irradiation. The optimum concentration of GNPs was evaluated in our previous study (14).

Evaluation of stemness parameters

Flow cytometry: CD133 expression was assessed in single cell suspensions of HT29 CSLCs and parental cells. Briefly, the cells were washed twice with PBS and suspended in the sample buffer (PBS, 0.5% BSA and 2mMEDATA). After adding FCR blocking reagent and anti CD133 (CD133/PE Human monoclonal, Miltenyi Biotech), the samples were mixed and incubated in the dark for 30 min at 40C.The analysis was performed with FACS caliber (BD Biosciences, USA) using the Cell Quest software.

Quantitative real-time, reverse transcription PCR (qRT-PCR): Relative gene expression were analyzed using qRT-PCR. Total RNA was extracted from HT29 CSLCs and parental cells using GeneAll RiboEx kit (GeneAll Biotechnology, Korea) according to the manufacturer's protocol. Complementary DNA (cDNA) was synthesized using the SuperScript II reverse transcriptase (Invitrogen). qRT -PCR was performed with an ABI PRISM 7300 instrument (Applied Biosystems, US) using SYBR Green PCR Core Reagents (Thermo scientific). The primes used are shown in table S1. Standard curves were drown using serial dilution of pooled cDNA, including seven dilutions from 1/10 to 1/1000. The PCR efficiency was calculated using Eq.1

Eq.1 $E\% = 10(1 / \text{Slope}) - 1 \times 100$ (22)

The change in relative mRNA expression of stemness genes (23,24), Nanog, Oct4, c-MYC and CD133, was assessed using the standard curve method (25). All samples were normalized to GAPDH gene expression as the internal control.

Irradiation

Irradiation was performed using a clinical accelerator (Neptun 10 PC) at source-to-surface distance (SSD) = 100 cm, and 20 × 20 cm^2 field size. Two centimeters of a Plexiglass sheet (PMMA) was placed on the top of the plate to serve as a built-up material for the 9 MV beam. The plate was placed in a phantom made of Plexiglass with a sized cavity of 12.5×8.5×1.5 cm^3 at the center (Fig S1). Mega-voltage radiation (9 MV) was delivered at a total dose of 2, 4, 6 and 8 Gy with a dose rate of 300 cGy min^{-1}. *In vivo* radiation diode dosimetry measurements were done for the beam calibration and the variation within a field was smaller than 2% for each well. After irradiation, cells were incubated at 37°C, 5% CO_2.

Clonogenic assay

Survival fraction was determined based on colony formation assay. Cells were seeded in 6 well plate before irradiation. Fifteen day after irradiation, the cells were rinsed with PBS, fixed and stained with 4% paraformaldehyde solution, Hematoxylin &Eosin stain, respectively. Colonies with more than 50 cells were counted in triplicate with Image Master 2D platinum software. The relative cell surviving fraction was calculated by dividing the number of colonies of treated cells by that of the control (26).

Radioresistance analysis

Radiobiological parameters: In order to analyze the radiobiology parameters two prevalent models (1.) **Linear Quadratic Model (**LQ-model) and (2.) **Multi-targets single hit Model** have been suggested in this study (27).

For a single acute dose, Radiation survival curve was fitted using aforementioned models. Eventually, α, β, Mean Inactivation Dose (MID), n and D0 radiobiological parameters were calculated using Eq 2, 3 and 4. In presence of GNPs, the sensitivity enhancement ratio (SER) value and the RBE value at D10 (dose required to reduce the survival fraction to 10%), were calculated according to Eq.5,6 (6,8).

Eq.2 $S = exp\left(-(\alpha D + \beta D^2)\right)$

Eq.3 $MID = \int S(D)d(D)$

Eq.4 $S = 1 - (1 - e^{-D/D_0})^n$

Eq.5 $\mathrm{SER} = \mathrm{MID\ (X-ray)/MID\ (X-ray\ + GNPs)}$

Eq.6 $\mathrm{RBE} = \mathrm{D10\ (X-ray)/D10\ (X-ray\ + GNPs)}$

Cell cycle analysis: Cells were trypsinized and washed twice in PBS, then 10^6 cells fixed overnight in 70 % ethanol at -20˚C. The cells were centrifuged, re-suspended in 0.5 ml Propidium iodide(PI) staining solution (containing 50 µgml−1 PI and 10 µgml-1 RNase) for 30 min at RT. Sample were analyzed using a FACS Calibur flow cytometer (BD Biosciences, USA). Cell cycle distribution was evaluated before irradiation and 24 hours after exposure to 2 and 6 Gy irradiation doses.

ϒ-H2AX detection by Immunofluorescence: Phosphorylation of histone H2AX is a quantitative biomarker for identification of DNA double strand breaks (DSBs) in a cell (28). HT29 CSLCs and parental cells were seeded into six-well tissue culture plates containing a sterilized cover glass and irradiated with 4 Gy of X-ray in presence and absence of GNPs. Cultures were fixed for 20 min with freshly 4% paraformaldehyde and permeabilized with 0.1% Triton X-100, 2 and 24 hours after irradiation. Cells were blocked with 5% BSA in PBS for 40 min at room temperature. The samples were incubated with anti-phospho-histone H2AX (Ser139, clone JBW301) mouse monoclonal IgG1 (Upstate) overnight at 4° C and followed by secondary antibodies Alexa Fluor1 488 donkey anti-mouse IgG (H + L) for 45min at room temperature. The cell nuclei were stained with 49, 6-diamidino-2-phenylindole (DAPI) for 10 min. The cover slips were mounted on microscope slides using Vectashield antifade (Vector Laboratories, Burlingame, CA) and examined with a fluorescence

microscope (Olympus, Magnification:100x objective). The number of ϒH2AX foci were counted in 25 nucleus, at least.

Statistical analysis

All values are expressed as means ± SD. Differences less than 0.05 ($p<0.05$) were considered statistically significant. All experiments were performed in triplicate and repeated at least three times.

Results

Serum-free medium unregulated expression of stemness genes and formed sphere like structures in HT29 colorectal cancer cells

It is conspicuous that differentiated carcinoma cells die a few days after incubation in serum free culture medium and the cells with stem cell features survive and grow as spheroid like structure (29). As showed in Fig. 1 sphere formation was started from the third day and spheres reached to maximum size after 10 days in Col/SFM. After approximately 10 days of culture, the spheres emerged like a ball, round with a smooth surface. Also, an SEM image revealed that they had a vaulted structure in Col/SFM (Fig. 2).

Fig. 1

Fig. 2

Flow cytometry analysis indicated that the proportion of CD133, as a specific surface marker for colon CSLCs, in parental HT29 cells was approximately 25%. However, in Col/SFM the percentage of CD133 in HT29 CSLCs was dramatically increased to 84% as shown in Fig. 3a

In qRT-PCR analysis, we found that the expression of stemness genes, Nanog, Oct4, c-MYC and CD133 was more highly unregulated in the HT29 CSLCs compared with the parental cells (P-value<0.05) (Fig. 3b).

Fig. 3

Cell cycle progression differs in HT29 CSLCs and parental cells

Cell cycle distribution is one of the intrinsic factors that affect the degree of radiosensitization. As displayed in fig. 4a, HT29 CSLCs had a significantly higher proportion of G0/G1 phase cells compared with parental cells ($P<0.05$), whereas G2/M phase proportion was significantly lower ($P<0.05$). This result indicated that HT29 CSLCs population are in quiescence state and , as a result, they are more radiation-resistant than their parental cells (30,31).

Radiation remarkably redistribute HT29 parental cell cycle but have less effect on CSLCs

Activation of cell cycle check point is one of the mechanisms of DNA damage repair (32). Figure. 4a shows that the cell cycle distribution for HT29 CSLCs and parental cells 48 hours after 2Gy and 6Gy irradiation. The results indicated that in parental cells a dose-dependent cell cycle delay at G2/M phase accompanied by a proportional decrease of cells in G_0/G1 phase. By contrast, less prominent G2 phase retardation was displaced in HT29 CSLCs at different radiation doses. In other words, under the same irradiation dose, cell cycle arrest effects of radiation on HT29 CSLCs were significantly weaker than those on parental cells and irradiation did not induce significant changes in the cell cycle phase distribution of HT29 CSLCs compared with parental cells (fig. 4b, c).

Fig. 4

Radiation in the presence of GNPs decrease the radioresistance of HT29 CSLCs

The radiosensitivity of HT29 CSLCs and parental cells in presence and absence of GNPs were analyzed using clonogenic assay. Cell survival curves and related radiobiological parameters are presented in Fig. 5 and Table 1, respectively. Compared with parental cells,

HT29 CSLCs have shown higher survival following irradiation in a wide dose range (P-value <0.05).

HT29 CSLCs and parental cells survival fraction at 2Gy became 91% and 71%, respectively (P-value<0.05). Shoulder of HT29 CSLCs survival curve (n) turned wider than parental cells. Extracted radiobiological parameters from dose response curve for MID, and D_0 were significantly higher than the observed in parental cells (P-value <0.05), whereas linear component of survival curve (α) was significantly smaller in HT29 CSLCs than parental cells

The survival fraction of HT29 CSLCs and parental cells in presence of GNPs significantly decreased rather than the irradiation alone. The SER value of HT29 CSLCs and parental cells were 1.8 and 1.4, respectively. Moreover, changes in linear component and shoulder of survival curve in presence of GNPs were evaluated. These parameters determine the type of irradiation-induced cell death and present the difference between high and low LET energy(33). Surprisingly, in presence of GNPs linear component of HT29 CSLCs significantly increased and shoulder of survival curve decreased, as expected for high LET energy (P-value<0.05)(33). We found that the RBE value of HT29 CSLCs and parental cells for X-ray + GNPs beam relative to X-ray alone at D_{10} level were about 1.6 and 1.27, respectively.

Fig. 5

Table. 1

Induction and persistence of DNA-DSBs in presence of GNPs were increased in both HT-29 CSLCs and parental cells.

DNA DSBs were investigated following 4Gy X-ray irradiation in HT29 CSLCs and parental cells by ϒ-H2AX assay. As shown in fig.6, the number of foci induced after 2h in parental cells was significantly higher than those induced in CSLCs ($p<0.05$). These results indicate that parental cells were more susceptible to DNA DSBs. In addition, the number of

persistence ϒ-H2AX foci 24h after irradiation, unrepairable DNA DSBs, in HT-29 CSLCs was lower than parental cells (P-value<0.05). **C**ompared to radiation alone in the presence of GNPs the number of ϒ-H2AX foci induced 2 and 24 hours after irradiation in both HT29 CSLCs and parental cells were significantly increased (P-value<0.05).

Fig. 6

Discussion

Based on the recent studies, CSLCs population is highly resistant to conventional radiation therapy (2,3,34). Thus, the purpose of this study is to evaluate the radiosensitization enhancement of CSLCs in the third most common malignancy, colon cancer (35), in the presence of GNPs and low LET irradiation (X-ray). To approach this goal, we used the HT29 as the most radioresistant colon cancer cell line (36,37). The HT29 CSLCs were firstly isolated and characterized; then, the intrinsic radioresitance properties were evaluated. Spheroid like structures in Col/SFM expressed CD133 surface marker by 84%. Similarly, the mRNA level of the stemness related genes such as CD133, Oct4, c-MYC and Nanog was relatively high. These results were in consistent with previous reports that used SFM medium for CSLCs enrichment (19,20,29).

The intrinsic radio responsiveness of HT29 CSLCs was investigated with clonogenic survival curves. As it was shown in the previous studies (38,39), low value of linear component (α) of survival curve indicated high intrinsic radioresistance, low induced lethal damage and low apoptosis stimuli. Therefore, aforementioned intrinsic characteristics have been expected for our spheroid like structures because $\alpha_{parental}$ was higher than α_{CSLCs} in HT29 cell line (see Fig 5 and table 1). Similarly, a high value of survival curve shoulder (n) observed in HT29 CSLCs (see Fig 5 and table 1), revealed high potential repair of sublethal and potential lethal

damage as it was previously reported (39,40). Consistently, ϒ-H2AX assay showed fewer susceptibility to DNA DSBs induction in HT29 CSLCs than parental cells at 2h after irradiation which suggests high radioresistance for HT29 CSLCs (41,42). Unrepairable DNA DSBs were determined 24 hours after irradiation by counting the number of persisted ϒ-H2AX foci (6,43) . The fewer number of persisted ϒ-H2AX foci in HT29 CSLCs indicates a larger DSBs restoration capacity than parental cells (6,44–46).

Therefore, more complex DNA DSBs such as those occurred in high LET-irradiation are needed for HT29 CSLCs eradication. Furthermore, the cell cycle distribution before and after irradiation as a key parameter of intrinsic radio responsiveness (47) was also investigated. Before irradiation, HT29 CSLCs had higher G0/G1 and lower G2/M phase proportion compared to its parental cells. This may indicate that they are relatively quiescent and have slow cycling rate as was previously reported for CSLCs (39,48). Quiescent state precipitates an intrinsic defense mechanism that enables CSLCs to be resistant to therapeutic approaches targeting rapidly dividing cells(49). Forty-eight hours after irradiation, there was no obvious change in the cell cycle distribution of HT29 CSLCs; however, the population of cells in G2 phase was significantly increased in parental cells (Fig 4). The remarkable ability in repairing irradiation damages may enable CSLCs to pass checkpoint arrests more rapidly than parental cells (50). Consequently, in line with previous reports (39,48), our results suggest that alternation in the checkpoint response might allow HT29 CSLCs to circumvent the proapoptotic effects of radiation therapy and finally causes a decrease in cell death and an increase in proliferation activity.

CSLCs properties such as propensity to quiescence, enhanced DNA repair, unregulated cell cycle control systems and free radical scavenging mechanisms are able to tolerate the effects of treatments such as low LET irradiation in which the production of free radicals causes sub-lethal and potential lethal damage (40,51). Controversially, a direct action with high LET

irradiation predominantly induces clustered unrepairable DNA damages that finally increases RBE and decreases cell-cycle-dependent radiosensitivity (52,53). In this study, we showed that the combination of GNPs with X-ray energy can enhance radiosensitization of HT29 CSLCs. The results revealed that GNPs significantly increase α and decrease n components of survival curve due to an increased absorbed dose. Additionally, unrepairable DNA DSBs in CSLCs significantly were increased in the presence of GNPs. These results may be consistent with the expected high LET irradiation effects (6,33,54).

The most characteristic that distinguished high-LET radiation from low-LET radiation is induction of more serious DNA DSBs, described by higher value of the relative biological effectiveness (55,56). The colony assay of HT29 parental cells showed the RBE values of 1.27 *in vitro* at D10 for X-ray + GNPs (Table1). In previous studies (54,57), using HIMAC carbon-ion beams the RBE value of 1.06 to 1.33 for a 13-keV/mm-beam on different cancer cell lines such as brain, pancreas and lung tumors was reported. Furthermore, the RBE value of HCT116 and Sw480 colon cancer cell lines for a SOBP carbon ion beam, was reported 1.63 and 1.74 for a 50-keV/mm-beam, respectively (2). These results suggested that the calculated RBE value induced by GNPs+X-ray may be almost in consistent with the range of 13-keV/mm-beam carbon-ion. Additionally, RBE value calculated at the D10 level for HT29 CSLCs was about 1.6 that significantly was higher than parental cells. Theoretically, these findings can be explained by new nanodosimetric models (12,58,59). In the presence of GNPs, production of Auger electrons with low energy and small range results in highly inhomogenous dose distributions on the nanoscale. Therefore, in parallel with previous studies targeted CSLCs with heavy ion (2,6,8,10), it can be implied that the GNPs+X-ray induces more complex DNA damages compare to X-ray due to higher RBE value of HT29 CSLCs than parental cells . Moreover, these results can suggest that the combination has a promising potential to destroy HT29 cancer stem–like cells.

The results of survival curves indicated that this has an advantage over X-rays to target HT29 CSLCs. Thus, this method can be considered as an alternative for high LET therapy; however, further evaluation in *in vivo* conditions is required.

Acknowledgements

The authors are highly thankful to all technicians who provided support during the course of research. The part of this work was supported by Stem Cell Research Center, Golestan University of Medical Science (Grant no: 950818185).

Disclosure statement

No potential conflict of interest was reported by the authors

References

1. Roy S, Majumdar AP. Signaling in colon cancer stem cells. J Mol Signal 2012;7(1):11.

2. Cui X, Oonishi K, Tsujii H, Yasuda T, Matsumoto Y, Furusawa Y, et al. Effects of carbon ion beam on putative colon cancer stem cells and its comparison with X-rays. Cancer Res 2011;71(10):3676–87.

3. Moncharmont C, Levy A, Gilormini M, Bertrand G, Chargari C, Alphonse G, et al. Targeting a cornerstone of radiation resistance: cancer stem cell. Cancer Lett 2012;322(2):139–47.

4. Kahlert UD, Mooney SM, Natsumeda M, Steiger H-J, Maciaczyk J. Targeting cancer stem-like cells in glioblastoma and colorectal cancer through metabolic pathways. Int J Cancer 2017;140(1):10–22.

5. Okayasu R, Okada M, Okabe A, Noguchi M, Takakura K, Takahashi S. Repair of DNA damage induced by accelerated heavy ions in mammalian cells proficient and deficient in the non-homologous end-joining pathway. Radiat Res 2006;165(1):59–67.

6. Hirota Y, Masunaga SI, Kondo N, Kawabata S, Hirakawa H, Yajima H, et al. High linear-energy-transfer radiation can overcome radioresistance of glioma stem-like cells to low linear-energy-transfer radiation. J Radiat Res 2014;55:75–83.

7. Oonishi K, Cui X, Hirakawa H, Fujimori A, Kamijo T, Yamada S, et al. Different effects of carbon ion beams and X-rays on clonogenic survival and DNA repair in human pancreatic cancer stem-like cells. Radiother Oncol 2012;105(2):258–65.

8. Takahashi M, Hirakawa H, Yajima H, Izumi-Nakajima N, Okayasu R, Fujimori A. Carbon ion beam is more effective to induce cell death in sphere-type A172 human glioblastoma cells compared with X-rays. Int J Radiat Biol 2014;90:1125–32.

9. A. Takahashi, H. Ma, A. Nakagawa, Y. Yoshida, T. Kanai, T. Ohno,et al. Carbon-Ion Beams Efficiently Induce Cell Killing in X-Ray Resistant Human Squamous Tongue Cancer Cells. Int J Med Phys Clin Eng Radiat Oncol 2014;(3):133–42.

10. Sai S, Vares G, Kim EH, Karasawa K, Wang B, Nenoi M, et al. Carbon ion beam combined with

cisplatin effectively disrupts triple negative breast cancer stem-like cells in vitro. Mol Cancer 2015;(3):1–13.

11. Niemantsverdriet M, van Goethem MJ, Bron R, Hogewerf W, Brandenburg S, Langendijk JA, et al. High and Low LET Radiation Differentially Induce Normal Tissue Damage Signals. Radiat Oncol Biol 2012;83(4):1291–7.

12. McMahon SJ, Hyland WB, Muir MF, Coulter J a, Jain S, Butterworth KT, et al. Biological consequences of nanoscale energy deposition near irradiated heavy atom nanoparticles. Sci Rep 2011;1:18.

13. Jain S, Coulter JA, Hounsell AR, Butterworth KT, McMahon SJ, Hyland WB,et al. Cell-specific radiosensitization by gold nanoparticles at megavoltage radiation energies.Int J Radiat Oncol Biol Phys 2011;79(2):531–9.

14. Saberi A, Shahbazi-Gahrouei D, Abbasian M, Fesharaki M, Baharlouei A, Arab-Bafrani Z. Gold nanoparticles in combination with megavoltage radiation energy increased radiosensitization and apoptosis in colon cancer HT-29 cells. Int J Radiat Biol 2016;1–9.

15. Chithrani DB, Jelveh S, Jalali F, van Prooijen M, Allen C, Bristow RG, et al. Gold nanoparticles as radiation sensitizers in cancer therapy. Radiat Res 2010;173(6):719–28.

16. Butterworth KT, Coulter JA, Jain S, Forker J, McMahon SJ, Schettino G, et al. Evaluation of cytotoxicity and radiation enhancement using 1.9 nm gold particles: potential application for cancer therapy. Nanotechnology 2010;21(29):295101.

17. Chattopadhyay N, Cai Z, Kwon YL, Lechtman E, Pignol JP, Reilly RM. Molecularly targeted gold nanoparticles enhance the radiation response of breast cancer cells and tumor xenografts to X-radiation. Breast Cancer Res Treat 2013;137(1):81–91.

18. Arab-bafrani Z, Shahbazi-gahrouei D, Abbasian M, Saberi A, Fesharaki M. Culturing in serum-free culture medium on collagen type-I-coated plate increases expression of CD133 and retains original phenotype of HT-29 cancer stem cell. Adv Biomed Res 2016 22;5:59

19. Fang DD, Kim YJ, Lee CN, Aggarwal S, McKinnon K, Mesmer D, et al. Expansion of CD133(+) colon cancer cultures retaining stem cell properties to enable cancer stem cell target discovery. Br J Cancer 2010;102(8):1265–75.

20. Kirkland SC. Type I collagen inhibits differentiation and promotes a stem cell-like phenotype in human colorectal carcinoma cells. Br J Cancer 2009;101(2):320–6.

21. Girard YK, Wang C, Ravi S, Howell MC, Mallela J, Alibrahim M, et al. A 3D Fibrous Scaffold Inducing Tumoroids: A Platform for Anticancer Drug Development. PLoS One 2013 ;8(10):e75345.

22. Radonic A, Thulke S, Mackay IM, Landt O, Siegert W, Nitsche A. Guideline to reference gene selection for quantitative real−time PCR. Biochem Biophys Res Commun 2004;313(4):856-62.

23. Rao G, Liu H, Li B, Hao J, Yang Y, Wang M, et al. Establishment of a human colorectal cancer cell line P6C with stem cell properties and resistance to chemotherapeutic drugs. Acta Pharmacol Sin 2013;34(6):793–804.

24. Botchkina GI, Zuniga ES, Das M, Wang Y, Wang H, Zhu S, et al. New-generation taxoid SB-T-1214 inhibits stem cell-related gene expression in 3D cancer spheroids induced by purified colon tumor-initiating cells. Mol Cancer 2010;9:192.

25. Larionov A, Krause A, Miller W. A standard curve based method for relative real time PCR data processing. BMC Bioinformatics. BMC Bioinformatics 2005;6(1):62.

26. Chen W-S, Lee Y-J, Yu Y-C, Hsaio C-H, Yen J-H, Yu S-H, et al. Enhancement of p53-mutant human colorectal cancer cells radiosensitivity by flavonoid fisetin. Int J Radiat Oncol Biol Phys 2010;77(5):1527–35.

27. Weichselbaum RR, Beckett MA, Vijayakumar S, Simon MA, Awan AM, Nachman J, et al. Radiobiological characterization of head and neck and sarcoma cellsderived from patients prior to rafiotherapy. Int J Radiat Oncol Biol Phys 1990;19:313–9.

28. Ismail IH, Wadhra TI, Hammarsten O. An optimized method for detecting gamma-H2AX in blood cells reveals a significant interindividual variation in the gamma-H2AX response among humans. Nucleic Acids Res 2007;35(5): e36.

29. Wei B, Han X-Y, Qi C-L, Zhang S, Zheng Z-H, Huang Y, et al. Coaction of spheroid-derived stem-like cells and endothelial progenitor cells promotes development of colon cancer. PLoS One 2012;7(6):e39069.

30. Sun L, Cabarcas SM. Radioresistance and Cancer Stem Cells: Survival of the Fittest. J Carcinog Mutagen 2012;1(S1):1–12.

31. Moore N, Lyle S. Quiescent, slow-cycling stem cell populations in cancer: a review of the evidence and discussion of significance. J Oncol 2010; 2011(2011):11.

32. Wiskirchen J, Dittmann H, Kehlbach R, Vogel-Claussen J, Gebert R, Dohmen BM, et al. Rhenium-188 for inhibition of human aortic smooth muscle cell proliferation. Int J Radiat Oncol Biol Phys 2001;49(3):809–15.

33. Hall EJ; Linear Energy Transfer and Relative Biologic Effectiveness,Charles W, Radiobiology for the Radiologist, seventh ed, New York, Wolters kluwer, (1988), pp106-108.

34. Nguyen GH, Murph MM, Chang JY. Cancer Stem Cell Radioresistance and Enrichment: Where Frontline Radiation Therapy May Fail in Lung and Esophageal Cancers. Cancers (Basel) 2011;3(1):1232–52.

35. Siegel R, DeSantis C, Jemal A. Colorectal cancer statistics, 2014. CA Cancer J Clin 2014 ;64(2):104–17.

36. Frykholm G, Glimelius B, Richter S, Carlsson J. Heterogeneity in antigenic expression and radiosensitivity in human colon carcinoma cell lines. In Vitro Cell Dev Biol 1991;27A(12):900–6.

37. Dunne AL, Price ME, Mothersill C, McKeown SR, Robson T, Hirst DG. Relationship between clonogenic radiosensitivity, radiation-induced apoptosis and DNA damage/repair in human colon cancer cells. Br J Cancer 2003;89(12):2277–83.

38. Parfitt SL, Milner RJ, Salute ME, Hintenlang DE, Farese JP, Bacon NJ, et al. Radiosensitivity and capacity for radiation-induced sublethal damage repair of canine transitional cell carcinoma (TCC) cell lines. Vet Comp Oncol 2011;9(3):232–40.

39. Martins-Neves SR, Lopes AO, Carmo A, Paiva A a, Simões PC, Abrunhosa AJ, et al. Therapeutic implications of an enriched cancer stem-like cell population in a human osteosarcoma cell line. BMC Cancer 2012;12(1):139.

40. Phillips TM, Mcbride WH, Pajonk F. The Response of CD24 − / low / CD44 + Breast Cancer – Initiating Cells to Radiation. J Natl Cancer Inst 2006;98(24):1777-85.

41. Cells GS, Jamal M, Rath BH, Tsang PS, Camphausen K, Tofilon PJ. The Brain Microenvironment Preferentially Enhances the. Neoplasia 2012;14(2):150–8.

42. Diehn M, Cho RW, Lobo NA, Kalisky T, Dorie MJ, Kulp AN, et al. Association of reactive oxygen species levels and radioresistance in cancer stem cells. Nature 2009;458(7239):780–3.

43. Schmid TE, Dollinger G, Beisker W, Hable V, Greubel C, Auer S, et al. Differences in the kinetics of γ-H2AX fluorescence decay after exposure to low and high LET radiation. Int J Radiat Biol 2010 ;86(8):682–91.

44. Taneja N, Davis M, Choy JS, Beckett MA, Singh R, Kron SJ, et al. Histone H2AX Phosphorylation as a Predictor of Radiosensitivity and Target for Radiotherapy. J Biol Chem 2004;279(3):2273–80.

45. Menegakis A, Yaromina A, Eicheler W, Dörfler A, Beuthien-Baumann B, Thames HD, et al. Prediction of clonogenic cell survival curves based on the number of residual DNA double strand breaks measured by γH2AX staining. Int J Radiat Biol 2009;85(11):1032–41.

46. Oonishi K, Cui X, Hirakawa H, Fujimori A, Kamijo T. Different effects of carbon ion beams and X-rays on clonogenic survival and DNA repair in human pancreatic cancer stem-like cells Radiother Oncol 2012 ;105(2):258-65.

47. Kim S, Rhee JG, Song X, Prochownik E V, Spitz DR, Lee YJ. Breast Cancer Stem Cell-Like Cells Are More Sensitive to Ionizing Radiation than Non-Stem Cells : Role of ATM. PLoS One 2012;7(11):e50423.

48. Lundholm L, Haag P, Zong D, Juntti T, Mörk B, Lewensohn R,et al. Resistance to DNA-damaging treatment in non-small cell lung cancer tumor-initiating cells involves reduced DNA-PK / ATM activation and diminished cell cycle arrest. Cell Death Dis 2013;4:e478.

49. Diaz A, Leon K. Therapeutic approaches to target cancer stem cells. Cancers (Basel) 2011;3(3):3331–52.

50. Eyler CE, Rich JN. Survival of the fittest: cancer stem cells in therapeutic resistance and angiogenesis.

J Clin Oncol 2009;26(17):2839–2845.

51. Escherichia R, Billen D. Free Radical Scavenging and the Expression of Potentially Lethal Damage in X-lrradiated Repair-Deficient Escherichia coli. Radiat Res 2014;111(2):354–60.

52. Okayasu R. Repair of DNA damage induced by accelerated heavy ions,a mini review Int J Cancer 2012;1000:991–1000.

53. Hada M, Georgakilas AG. Formation of clustered DNA damage after high-LET irradiation: a review. J Radiat Res 2008;49(3):203–10.

54. Suzuki M, Kase Y, Yamaguchi H, Kanai T, Ando K. Relative biological effectiveness for cell-killing effect on various human cell lines irradiated with heavy-ion medical accelerator in Chiba (HIMAC) carbon-ion beams. Int J Radiat Oncol 2000;48(1):241–50.

55. Goodhead DT. Mechanisms for the biological effectiveness of high-LET radiations. J Radiat Res 1999;40 Suppl:1–13.

56. Goodhead DT. Initial events in the cellular effects of ionizing radiations : clustered damage in DNA. Int J Radiat Biol 1994;65(1):7-17.

57. Matsui Y, Asano T, Kenmochi T, Iwakawa M, Imai T, Ochiai T. Effects of carbon-ion beams on human pancreatic cancer cell lines that differ in genetic status. Am J Clin Oncol 2004;27(1):24–8.

58. McMahon SJ, Hyland WB, Muir MF, Coulter J a, Jain S, Butterworth KT, et al. Nanodosimetric effects of gold nanoparticles in megavoltage radiation therapy. Radiother Oncol 2011;100(3):412–6.

59. Gadoue SM, Toomeh D, Zygmanski P, Sajo E. Angular dose anisotropy around gold nanoparticles

exposed to X-rays. Nanomedicine Nanotechnology, Biol Med 2017;13(5):1653–61.

Table:

Table 1. Radiobilogical parameters of HT29 CSLCs and parental cells after irradiation

Parameters	Parental cells	CSLCs	Parental cells +GNPS	CSLCs+ GNPs
SF_2	75%	92%	56%	78%
α	0.14	0.03	0.25	0.1
MID	5.02	10.39	3.61	5.8
n	1.6	2.2	1.1	1.8
D_0	3.4	5.1	3.2	4.5
D_{50}	4.29	10	2.68	5
SER	–	–	1.4	1.8
RBE	–	–	1.27	1.6

Figurs:

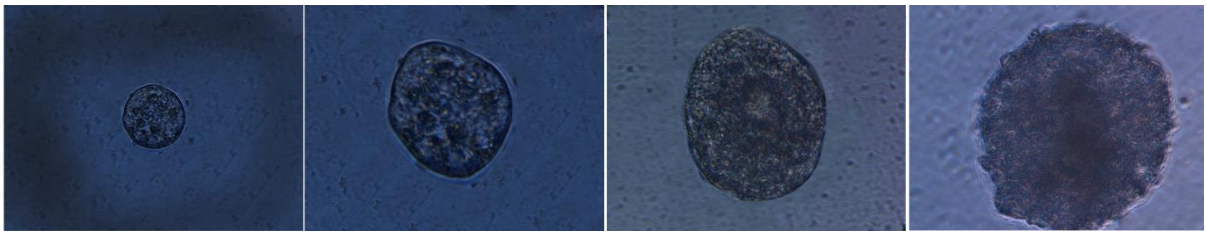

Day 3 **Day 6** **Day 8** **Day 10**

Figure 1.

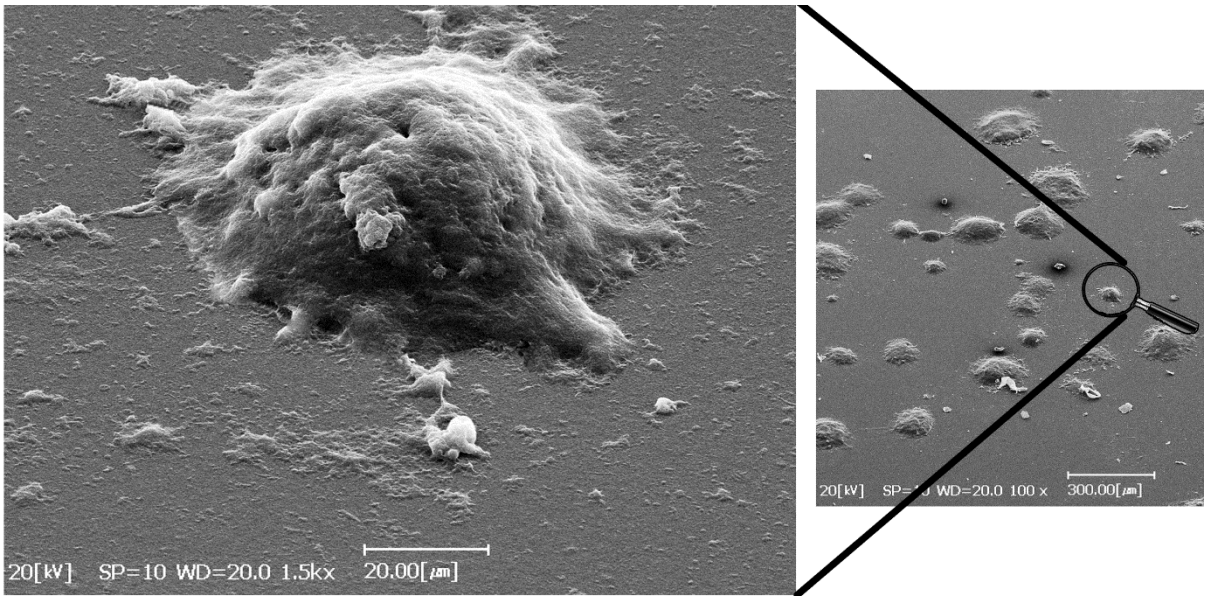

Figure 2.

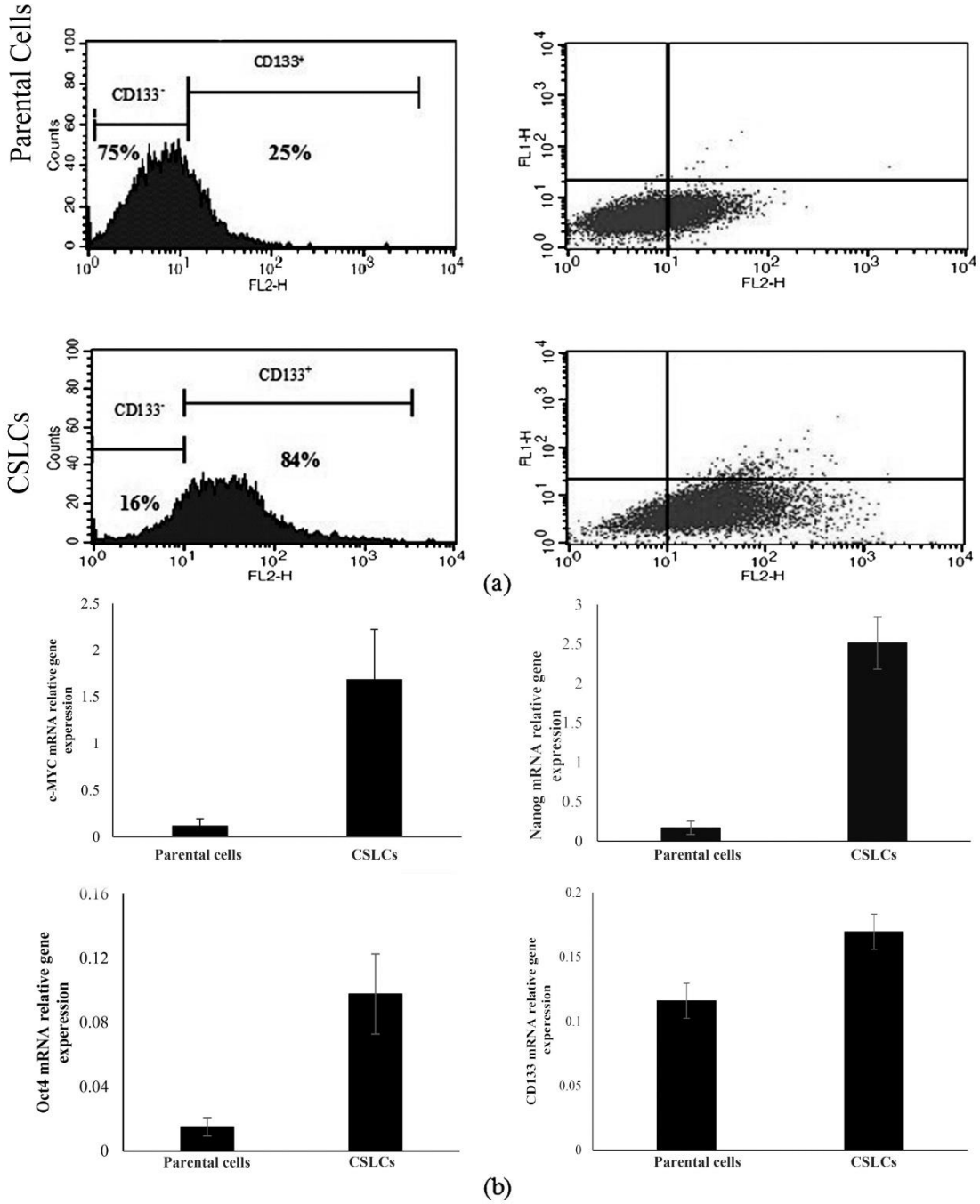
Parental Cells
CD133+
CD133-
75%
25%
Counts
FL2-H
FL1-H
CSLCs
CD133+
CD133-
84%
16%
(a)
c-MYC mRNA relative gene experession
Nanog mRNA relative gene expression
Oct4 mRNA relative gene experession
CD133 mRNA relative gene experession
Parental cells
CSLCs
(b)

Figure 3.

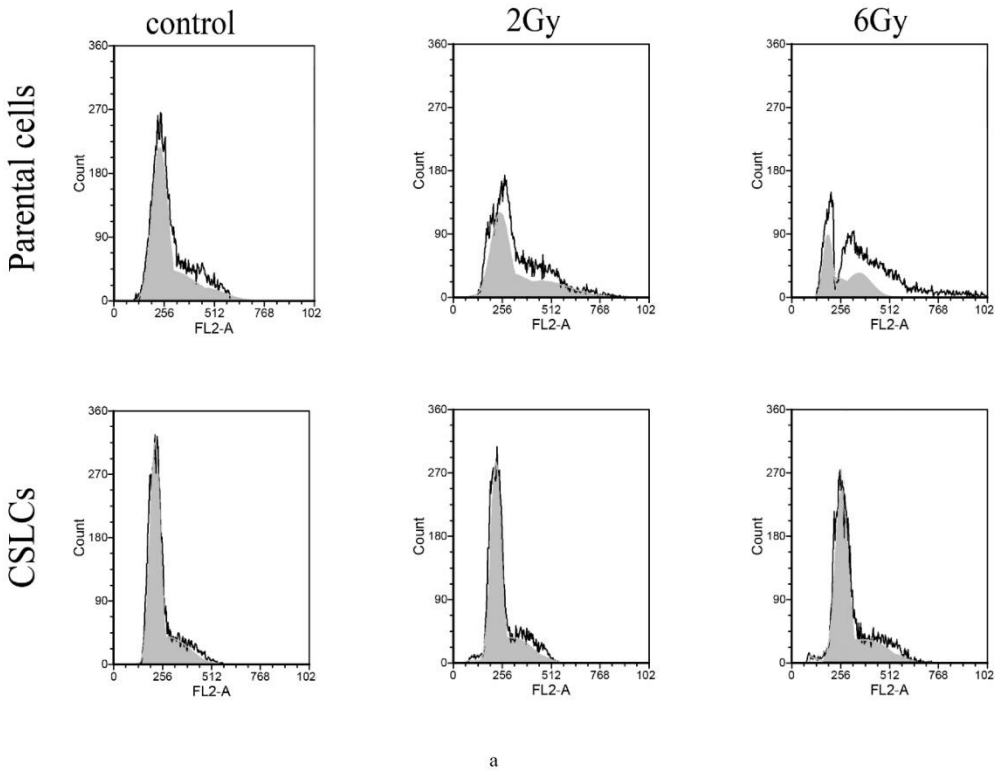
control
2Gy
6Gy
Parental cells
CSLCs
Count
FL2-A
a
Cell Population in G0/G1 phase (%)
parental cells
CSLCs
control
Irradiation(2Gy)
Irradiation(6Gy)
b
Cell population in G2/M phase(%)
Parental cells
CSLCs
control
Irradiation(2Gy)
Irradiation(6Gy)
c

Figure. 4

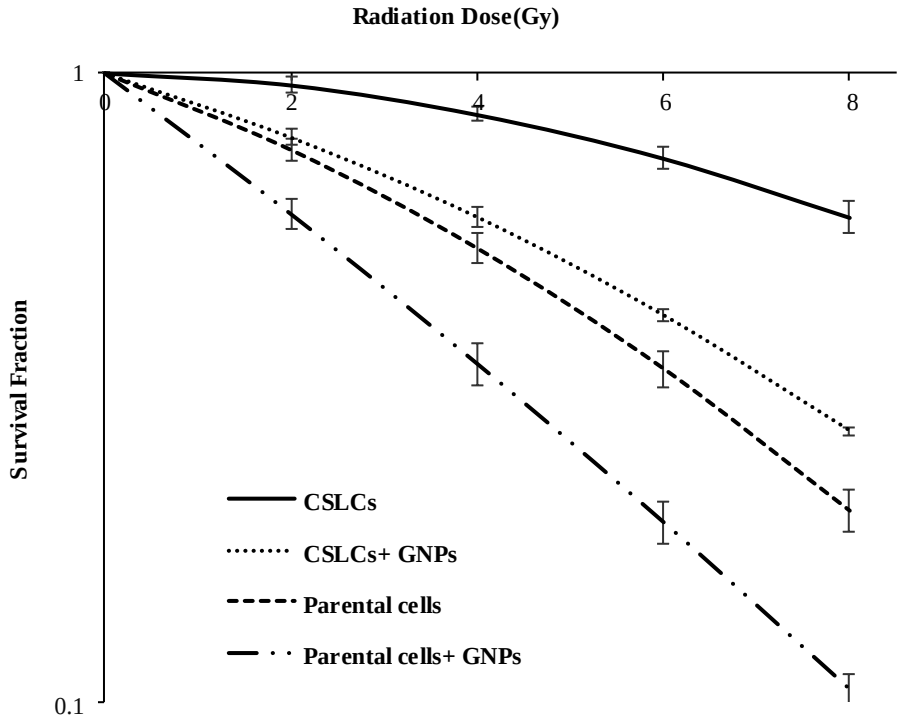
Radiation Dose(Gy)
1
0
2
4
6
8
0.1
Survival Fraction
CSLCs
CSLCs+ GNPs
Parental cells
Parental cells+ GNPs

Figure 5.

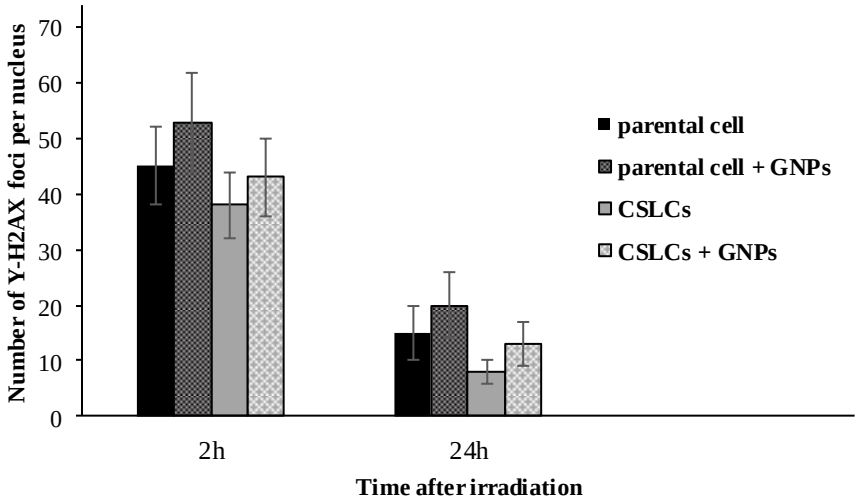
Number of γ-H2AX foci per nucleus
70
60
50
40
30
20
10
0
2h
24h
Time after irradiation
parental cell
parental cell + GNPs
CSLCs
CSLCs + GNPs

Figure 6.

Figure legend:

Figure 1. Inverted optical microscopy showed the growth of spheroid liked structure that formed in Col/SFM (Magnification: 40x objective).

Figure 2. SEM images of HT-29 spheroid like structure after 10 days of culture in Col/SFM

Figure 3 Expression of CD133 surface marker (a) and stemness genes (b) in HT-29 CSLCs and parental cells

Figure 4. Cell cycle analysis of HT29 CSLCs and parental cells before and after irradiation with different radiation deses. (a) Distribution of cell population to different cell cycle phases were analyzed using flow cytometry analysis. (b), (c) column graph showing the results from flow cytometry analysis.

Figure 5. The dose responsive curves of HT29 CSLCs and parental cells in presence and absence of GNPs

Figure 6. The number of γH2AX foci in HT-29 CSLCs and Parental cells after 4Gy irradiation in presence and absence of GNPs